Construction and Building Materials 411 (2024) 134397

Contents lists available at ScienceDirect

Construction and Building Materials

journal homepage: www.elsevier.com/locate/conbuildmat

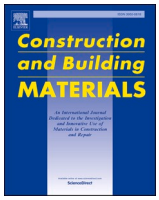

Acid attack on alkali-activated mortars: A test proposal

A. Mellado-Romero, J. Martín-Rodríguez, M.V. Borrachero, L. Soriano, J.M. Monzó, J. Payá *

Grupo de Investigación en Química de los Materiales (GIQUIMA), Instituto de Ciencia y Tecnología del Hormigón (ICITECH), Universitat Politècnica de València, Camino de Vera s/n, E-46022 Valencia, Spain

A R T I C L E I N F O

Keywords:
Acid attack
Nitric acid
Alkali-activated mortars
Acid neutralization capacity
Mass loss
Thermogravimetry

A B S T R A C T

The durability of new binders in construction is one of the keys for further applications. The acid attack resistance of alkali-activated mortars (AAMs) was tested. A test proposal was developed, and the selected AAMs (precursors: blastfurnace slag, vitreous calcium silicoaluminate, fly ash and spent FCC catalyst) were analyzed in terms of acid neutralization capacity (ANC), mass loss at a constant pH= 2, and mass loss of the cubes immersed in 1 molar nitric acid solution. The results were compared to the mortars prepared with ordinary Portland cement. The ANC values were generally higher when the calcium content of the binder increased. The attacked mortars were characterized by thermogravimetry and microscopy techniques. The proposed test, based on three complementary experiments, allows the analysis of AAMs' stability and the identification of more resistant systems to acid attack.

1. Introduction

Current construction needs require large amounts of binders with good physico-mechanical performance and the slightest possible environmental impact. today, alkali-activated binders (AABs) are one of the best possible options.

Alkali-activated binders, also called geopolymers by some authors, are composed of an aluminosilicate raw material (precursor) in an amorphous state and a highly concentrated alkaline activator (usually alkali silicate-hydroxide solution). The reaction yields a three-dimensional inorganic polymer network (N-A-S-H gel, or is alternately mixed with C-A-S-H gel when calcium is present in the system), which contributes to the high compressive strength of the hardened product [1].

Traditionally, AABs are prepared from metakaolin (MK), fly ash (FA) or ground granulated blast-furnace slag (GGBS) as aluminosilicate-source materials [2,3]. The use of waste in AAB systems has several advantages. First, it provides a sustainable solution for disposing of waste material that would otherwise be sent to landfills. Second, it reduces the need to produce Portland cement, which is a significant source of carbon dioxide emissions.

Research [4,5] has shown that the properties of the AABs made with FA can be affected by factors like the type and amount of employed activator, curing temperature and time, and the particle size and chemical composition of FA. Therefore, optimizing the production process is important for obtaining the desired properties. The FA/activator mixture is heated and allowed to react, which leads to the formation of N-A-S-H (sodium aluminosilicate hydrate) gel [6]. This gel can have a three-dimensional gel-like structure, which typically comprises similar chains of linked tetrahedral units to the structure of zeolites. The exact gel structure can vary depending on the specific FA composition, the type and concentration of the alkali activator, and the reaction conditions [7].

GGBS can be easily activated because it possesses hydraulic reactivity. A low concentration of NaOH and/or sodium silicate is usually required for good GGBS activation [8]. The C-A-S-H (calcium aluminosilicate hydrate) gel formed from the activation of blast furnace slag in AABs is similar to the C-S-H (calcium silicate hydrate) gel that is produced in Portland cement-based materials. However, the C-A-S-H gel contains a higher proportion of aluminum and has a slightly different atom arrangement structure than the C-S-H gel. The C-A-S-H gel is formed by the reaction among the calcium, silicon and aluminum oxides present in the blast furnace slag and the alkaline activator. The alkaline activator provides the necessary hydroxide ions to initiate the reaction and promotes blast furnace slag dissolution [9].

There are many examples of geopolymers prepared from various industrial or agricultural byproducts or waste materials. For example, Tashima et al. [10] developed a new geopolymeric binder based on fluid catalytic cracking catalyst residue (FCC). They obtained a compressive strength of 68 MPa for a mortar with a 1.19 SiO_2/Na_2O molar ratio (in

* Corresponding author.
E-mail address: jjpaya@cst.upv.es (J. Payá).

https://doi.org/10.1016/j.conbuildmat.2023.134397
Received 28 July 2023; Received in revised form 15 November 2023; Accepted 29 November 2023
Available online 12 December 2023

Table 1
Chemical composition of the employed materials (*LOI: Loss on ignition).

Oxide (%)	CaO	SiO_2	Al_2O_3	Fe_2O_3	MgO	SO_3	Na_2O	K_2O	Other	LOI*
OPC	63.98	18.54	3.74	2.78	2.14	4.41	0.37	1.11	0.96	1.95
GGBS	40.15	29.89	10.55	1.29	7.43	1.93	0.87	0.57	1.15	—
VCAS	23.51	57.90	12.92	0.47	2.88	—	0.74	0.13	1.20	0.25
FA	3.84	49.91	25.80	13.94	1.06	1.00	—	2.47	—	1.97
FCC	0.11	47.76	49.26	0.60	0.17	0.02	0.31	0.02	1.23	0.51

the activator reagent) cured for 3 days at 65 °C. The same authors proposed vitreous calcium aluminosilicate (VCAS) derived from glass fiber waste to act as the precursor to prepare an AAB, which provides compressive strength close to 89 MPa after curing 360 days at room temperature [11].

One fundamental aspect of using these binders is their durability, specifically in acidic environments. Binders based on Portland cement clinker normally well resist acidic environments [12]. Geopolymeric concretes must be able to maintain their properties against the possible attacks of external agents, such as acids, alkalis, chlorides, sulfates, atmospheric CO_2, among others. Specifically acid attack on concrete can occur in various scenarios, as in industrial or agricultural environments, and also in urban activity. Ordinary Portland cement- (OPC) based materials are very susceptible to being attacked by acids due to their high calcium content and the significant solubility of portlandite, Ca $(OH)_2$ [13]. The acid neutralization capacity of OPC at pH 6 is 18 mmol/g [14], but is lower for blended cements (*e.g.* 10 mmol/g for the blast furnace slag/OPC 1:4 system). Calcium aluminate cement (CAC) and high ye'elimite calcium sulfoaluminate cement (CSA-HY) hydrates are more reactive to acid: Damion and Chaunsali [15] demonstrated that the mass loss and consumed sulfuric acids for these hydrated pastes were significantly higher than that for OPC. However, CSA-HY and CAC performed better than OPC with citric acid at pH 3, probably due to the presence of portlandite in hydrated OPC.

Numerous studies confirm that geopolymers are more resistant to acid attack than OPC [16,17]. Mass loss and strength loss are the parameters that are commonly used to determine durability after immersing mortar or concrete specimens in acidic solutions. Mallikarjuna and Kireety [18] studied the behavior of GGBS+FA geopolymer mortars during attacks with sulfuric and nitric acids. They concluded that the tested mortars were less resistant to sulfuric acid than to nitric acid, and the most resistant was that containing only FA. The calcium content of a binder seems fundamental for its behavior against acids: the higher the calcium content, the less durability [17,18].

The same conclusion was reached by Mellado et al. [19], who determined the acid neutralization capacity (ANC) of powdered samples of OPC pastes and geopolymer pastes synthesized from GGBS, FA, FCC and ceramic waste (CW) as precursors. They generally observed that the ANC values were directly related to the calcium content of samples, and the same trend was noted for the mass loss of the monolithic paste samples immersed in nitric acid at pH 2.

A study [20] that compared the resistance of FA-based geopolymers against the action of H_2SO_4 and HNO_3 revealed that the mortar structure remained intact after coming into contact with H_2SO_4, while the HNO_3 solution slightly yellowed. In addition, the specimens with a lower Na_2O content lost their alkalinity more quickly than those with higher Na_2O contents in both attack types.

Lloyd et al. considered that the commonly used mass loss measure to determine resistance to acid attack in mortars was insufficient for showing their behavior in a "real environment", and could even lead to systematic errors [21]. The authors claimed that corroded depth was a more sensitive and accurate measurement, and provided more appropriate information about mortars' behavior against acid attacks.

Many of the previous studies on the ANC of cementing systems have been carried out on pastes. In the present study, the influence of sand in terms of the acid resistance of cementitious systems was analyzed. Analysis of the presence of additional interfaces (sand/paste) contributes to our understanding of the durability of alkali-activated systems. The studied mortars are related to either some microconcretes with quartz as a microaggregate or durable concretes for slabs designed for acidic environments in industrial structures. This paper presents a study of behavior against acid attack by HNO_3 under the different conditions of the selected alkali-activated mortars (AAMs) prepared from GGBS, VCAS, FA and spent fluid catalytic cracking catalyst of petroleum (FCC). Different methods were tested to assess the durability of these mortars in drastic acid attack situations and to make a comparison to the OPC control sample. First, the powdered samples of the prepared mortars were left at controlled 7, 4 and 2 pH values to calculate their ANC according to the specifications of Standard EA NEN 7371: 2004 [22]. After this test, adjusted modeling equations were obtained and proposed to analyze ANC *versus* time to predict mortars' behavior against acid attack. A thermogravimetric analysis (TGA) characterization of the attacked samples was also carried out. Additionally, variation in the mass *versus* time of mortar sheets was recorded by leaving them immersed in HNO_3 solutions at a constant pH 2. In this case, adjusted modeling equations were also obtained to describe the mass loss evolution *versus* time for these mortars. Optical microscopy and field emission scanning electron microscopy (FESEM) characterizations were also done on the attacked samples. Finally, another test was carried out by immersing cubic mortar specimens in HNO_3 solutions at pH 0 and recording both the mass variation of specimens and pH variation of the solution *versus* time.

2. Experimental section

2.1. Materials and apparatus

Table 1 shows the chemical composition of the OPC and raw materials used as the precursors of AABs (determined by X-ray fluorescence). OPC and GGBS were supplied by Cementval (Puerto de Sagunto, Spain), VCAS by Vitrominerals (Tennessee, USA), FA by Balalva (Onda, Spain) and FCC by BP Oil (Grao de Castellón, Spain). The density ($g{\cdot}cm^{-3}$) and fineness (mean particle diameter) of precursors were: OPC (3.15 $g{\cdot}cm^{-3}$and 17 μm), GGBS (2.87 $g{\cdot}cm^{-3}$ and 26 μm), VCAS (2.61 $g{\cdot}cm^{-3}$and 12 μm), FA (2.69 $g{\cdot}cm^{-3}$and 21 μm), and FCC (2.48 $g{\cdot}cm^{-3}$and 17 μm) To prepare the mortar specimens, siliceous sand was used, which complied with the specifications of Standard UNE-EN 196–1. Sodium hydroxide pellets (98% purity, supplied by Panreac SA Spain) and sodium silicate solution (water glass; 28% SiO_2, 8% Na_2O and 64% H_2O, provided by Merck-Spain) were employed to prepare the activating solutions. Nitric acid (65% purity; supplied by Panreac SA, Spain) was utilized to prepare the attacking solutions.

ANCs (at pH 7, 4 and 2) and the mass loss *versus* time (at a constant pH of 2) studies were conducted in an 805 Dosimat Plus automatic titration system (from Metrohm) coupled to a Delta-DO9765T pH transmitter (from LabProcess).

The TGA characterization of samples after the ANC test was done in a TGA 850 Mettler-Toledo thermobalance using sealed and pin-holed 100 μL-aluminum crucibles in a nitrogen atmosphere within the 35–600 °C range at the 10 °C/min heating rate, and were compared to the corresponding unattacked samples.

The deterioration of the surface and subsurface regions of the mortar

Table 2
Mix compositions of the alkali-activated mortars (*SiO_2/Na_2O is the molar ratio in the activating solutions).

Alkali-activated mortar	Water/precursor ratio (g/g)	$[Na^+]$ (mol/kg of solvent)	SiO_2/Na_2O (mol/mol) *	Water glass/precursor ratio (g/g)
GGBS	0.40	7	1.56	0.469
VCAS	0.40	10	0.0	0
FA	0.40	13	1.12	0.625
FCC	0.45	10	1.17	0.563

sheets after immersion in HNO_3 solution at a constant pH of 2 for 120 h was studied by optical microscopy (Leica MZ APO) and FESEM (Jeol JSM-6300, the Aztec 3.3 SP1 software).

2.2. Preparing specimens

To prepare the OPC mortar samples, the sand/cement ratio was set at 3 and the water/binder ratio at 0.5. Mortar specimens (40 ×40×160 mm^3) and (40 ×40 ×40 mm^3) were cured at 23 ± 2 °C at high relative humidity (RH ~ 100%) for 28 days.

The activating solutions were prepared at least 1 h in advance and were left to cool to room temperature prior to use. Then they were mixed with precursors and sand to prepare mortars with a sand/precursor ratio of 3. Table 2 summarizes the composition of the prepared AAMs. The GGBS and FCC mortars were cured in the same way as the OPC mortars, while the VCAS and FA specimens underwent a previous curing process at 65 ± 2 °C (RH ~ 100%) for 7 days before being placed inside the humid chamber (23 ± 2 °C; RH ~ 100%) for a 21-day period until 28 curing days.

2.3. Testing samples

For the ANC tests, mortar fragments were ground in an agate mortar, sieved to a particle size of < 125 μm and dried at 65 °C for 2 h. After cooling in a dried atmosphere, 1 g was weighed, placed in a beaker and 50 mL of deionized water were added to it. The sample was maintained in suspension with the help of a magnetic stirring device with the rod spinning at 300 rpm. After 10 min of stirring, the test started by adding HNO_3 solution (1 M) from the dosimeter at a flow rate of 4 mL/min until pH reached the selected value of 7, 4 or 2. The added HNO_3 solution volume of *versus* time was recorded until pH remained constant for longer than 15 min with no acid addition by means of the automatic titration system. All the tests were carried out in triplicate. The total number of measured ANC curves was 45 (5 mortars x 3 tested pH values x 3 repetitions). After finishing tests, the resulting suspensions were then filtered at low pressure with paper filters (11 μm pore size). The resulting solid was analyzed by TGA.

The mass loss of mortars *versus* reaction time was performed with the same device used in the ANC studies. Mortar sheets of 40 × 40×10 mm^3 were obtained from the monolithic specimens of 40 × 40×160 mm^3. Sheets were suspended in 200 mL of deionized water with the help of a fishing line to allow liquid to surround them on all sides. pH was allowed to remain constant at 2 by adding HNO_3 (1 M) solution from the dosimeter. At the predetermined times, sheets were removed from solution and weighed. The added acid volume was also recorded *versus* time. The assay duration was 120 h per mortar type and was carried out in duplicate. Then the attacked mortars of the freshly fractured specimens were examined by optical microscopy and immediately revealed with phenolphthalein to observe the acid attack front. Finally, FESEM studies were carried out on the samples impregnated with epoxy resin, cut, polished and coated with carbon. Elemental mappings (EDS) of the polished cross-sections were also performed.

Studies on the mass loss of the cubic specimens (40 ×40×40 mm^3) at an initial pH of 0 were done by immersing six samples in 2.5 L of HNO_3 solution (1 M) and recording their mass variation and the pH variation in the solution *versus* the reaction time. Specimens were placed inside a suitable container supported on glass rods to allow so they were all completely immersed and surrounded by liquid on all sides. At the predetermined times, cubes were removed from solution and weighed. The pH value of solution was also recorded. The test lasted up to 60 days. After this time, specimens' compressive strength was measured and compared to the compressive strength for the pristine mortars (a mechanical strength test was performed in an universal test machine following the procedures described in Standard UNE-EN 196–1, using six cubes per measurement).

3. Results and Discussion

3.1. ANC studies

By way of example, the experimental ANC test results (expressed as mmol of H^+ per gram of mortar) for the OPC and VCAS mortars at pH 7,

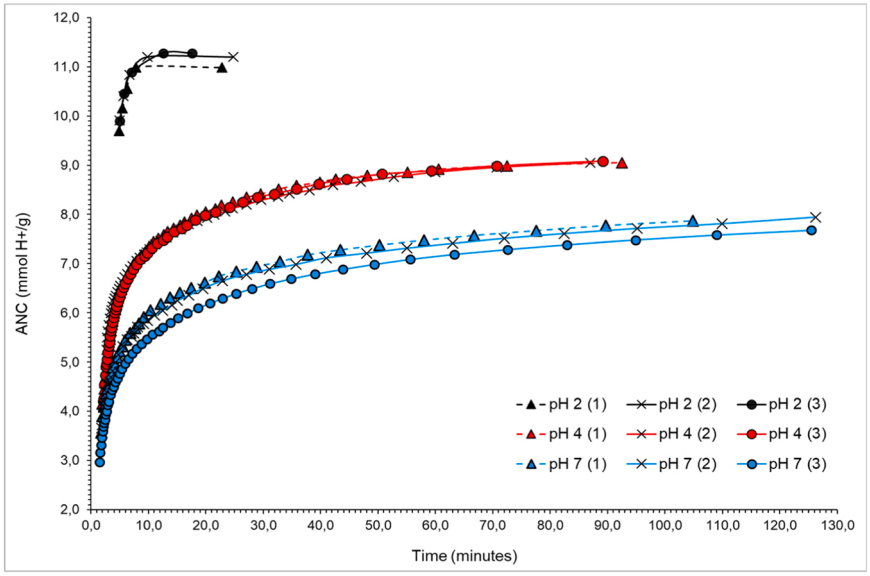

Fig. 1. ANC results for OPC at pH 2, pH 4 and pH 7 (three curves are represented because the test was done in triplicate).

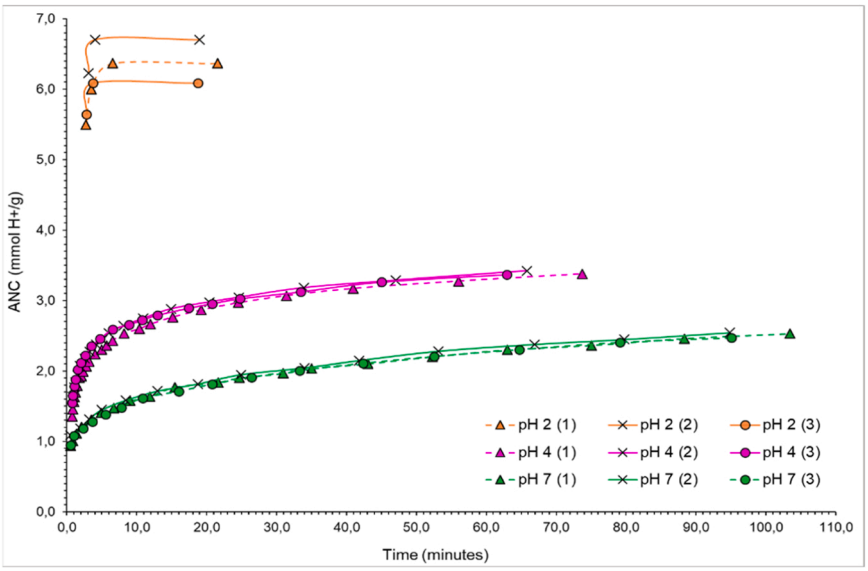

Fig. 2. ANC results for VCAS at pH 2, pH 4 and pH 7 (three curves are represented because the test was done in triplicate).

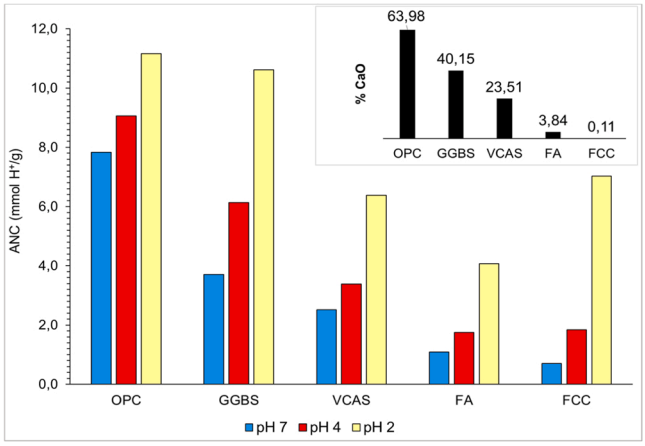

Fig. 3. ANC results for the OPC and alkali-activated mortars at pH 7, 4 and 2 (the %CaO content in binders is also shown).

4 and 2 are shown in Fig. 1 and Fig. 2.

For pH 2, the stabilization time was always shorter than 20 min. For pH 4 and 7, a time longer than 90 min for OPC, 80 min for GGBS, 70 min for VCAS, and 25 min for the FA and the FCC samples, were required.

Fig. 3 shows not only the average final values of the three ANC (expressed as mmol of H^+ per gram of mortar) tests per sample, but also the % CaO content of the binders used to prepare mortars.

For each binder type, the ANC values were higher at pH 2 than at pH 4, and these were higher than at pH 7. This is logical because more acid was required to neutralize the alkalinity of the initial medium (pH > 12) and to reach a lower pH value. It was also noted that, except for FCC at pH 2 and 4, the ANC values correlated proportionally to the calcium content in the binder. The OPC mortars consumed the biggest acid volume.

The ANC values for the OPC samples were 7.83, 9.06 and 11.16 mmol H^+/g for pH 7, 4 and 2, respectively. Portlandite's high solubility, and the presence of the largest quantities of hydrated calcium-based products (silicates and aluminates), were responsible for this sample's least resistance to acid attack.

The GGBS mortars had an ANC value at pH 7 (3.71), which was much lower than that of OPC, and the same behavior was observed at pH 4 (6.13). At pH 2, the value was similar: 10.61 mmol H^+/g of mortar.

Table 3
Experimental results of ANC and the parameters of the fitting equations of ANC *versus* time (R2 is the determination coefficient).

Mortar	pH	Final ANC (mmol H^+/g)	y_0	A_1	t_1	A_2	t_2	R^2
OPC	4	9.06	9.02	-9.25	1.47	-2.92	19.46	0.99
	7	7.83	7.74	-2.78	28.59	-4.14	1.94	0.97
GGBS	4	6.13	6.21	-1.95	40.82	-1.81	2.86	1.00
	7	3.71	3.71	-1.80	1.08	-1.36	16.95	0.99
VCAS	4	3.39	3.40	-1.23	20.71	-1.27	1.24	0.98
	7	2.51	2.73	-0.50	3.79	-1.31	55.26	1.00
FA	4	1.75	1.79	-0.92	0.44	-0.30	5.75	0.99
	7	1.09	1.15	-0.28	11.54	—	—	0.95
FCC	4	1.83	1.86	-0.47	6.56	-1.24	0.47	0.99
	7	0.69	0.69	—	—	—	—	1.00

These results demonstrate that the resistance to acid attack for the extreme conditions (pH 2) of both binders (OPC and GGBFS) was similar, while the hydration product of GGBS (C-A-S-H gel) was more resistant than that in the OPC system (C-S-H) under softer conditions (pH 4 and 7).

At pH 7, the VCAS, FA and FCC mortars followed the general trend: less calcium content and a lower value for the resulting ANC. However, FCC provided an abnormally high value of 7.03 mmol H^+/g at pH 2. We attributed this anomalous behavior to the N-A-S-H gel that formed during FCC hydration when decomposing after this intense acid attack. However in VCAS and FA (also with low calcium contents), the N-A-S-H gel remained stable, perhaps due to the different water/binder ratio used to prepare them: the FCC mortar was more susceptible to a very high acidic medium compared to the FA mortar (0.40 water/binder ratio). Such behavior was attributed to the higher water/binder ratio used to prepare the FCC-based mixture (0.45, see Table 2). Then with the *OriginPro8* program (© OriginLab Corporation, Northampton, Massachusetts, USA), a fit equation was obtained for ANC *versus* the time curves at pH 7 and 4 of the tested materials (at pH 2, there was no fit because of the few experimental points for some systems). The equation that was best fitted to describe the ANC behavior of mortars *versus* time is as follows:

$$y = y_0 + A_1 e^{-x/t_1} + A_2 e^{-x/t_2}$$

where y is ANC expressed as mmol H^+/g and x is the test time in

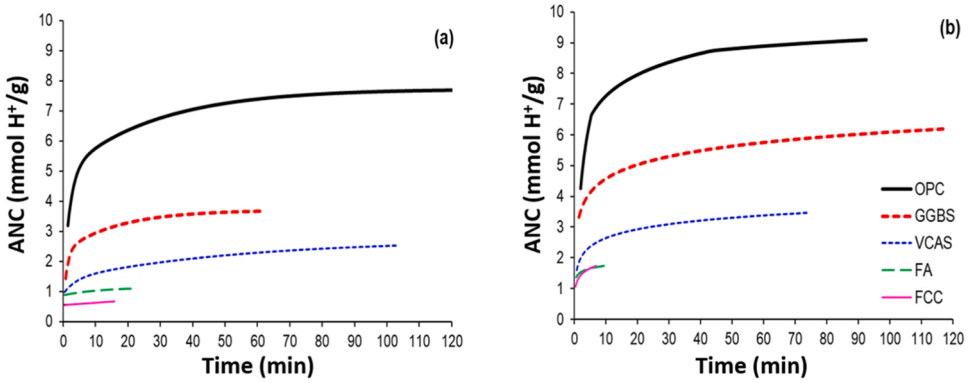

Fig. 4. Fitting curves of ANC *versus* time at (a) pH 7 and (b) pH 4.

minutes. Table 3 shows the values of the parameters corresponding to these curves for the mortars tested at pH 4 and 7. The shape of these curves is depicted n Fig. 4.

3.2. Thermal analysis

After finishing the ANC tests, the resulting suspensions were then filtered at low pressure. The resulting solids were washed with acetone and dried at 65 °C for 1 h. They were submitted to a TGA and compared to the corresponding unattacked samples.

Fig. 5**a** represents the first derivative (DTG) curves for the OPC mortars. Three main zones can be identified on the DTG curve corresponding to the control sample: the first one (centered at 150 °C) is attributable to the overlapped peaks of C-S-H and ettringite dehydrations; the second one (centered at 220 °C) corresponds to the dehydration of aluminates (C-A-H) and/or silicoaluminates (C-A-S-H); the third one (centered at 555 °C) is due to portlandite decomposition (loss of water). The total mass loss was 9.96% for this sample. After acid attack, the magnitude of all the peaks for samples lowered. In addition, the peak corresponding to CSH decomposition moved toward a lower temperature with a drop in pH. The peak at 555 °C was slight at pH 7 and practically disappeared at pH 4 and 2, which indicates that portlandite was completely leached during tests and C-S-H was partially decomposed, but more intensely when pH lowered.

The DTG curves for the GGBS mortars appear in Fig. 5**b**. The fact that no peak corresponded to portlandite on all the curves was remarkable (the peak at 580 °C for the sample treated at pH 2 was attributed to the carbonation products [23] that formed while handling the powdered sample). The peak related to C-S-H/C-A-S-H also moved toward lower temperatures, which suggests that this cementing phase was strongly affected by acid attack.

Fig. 5**c** shows the DTG curves for the VCAS sample, whose behavior was similar to GGBS, but the peak related to C-S-H (probably a mixture with N-A-S-H/C-A-S-H) was more marked at pH 4, which indicates the greater stability of these cementing phases.

The same peak centered at 150 °C is seen in Fig. 5**d** for the FA sample. In this case however it is worth mentioning the lower TGA mass loss values at pH 7 (5.10%) and pH 4 (5.79%) than in the other samples. Given the precursor's nature, the main formed hydrate was N-A-S-H [1]. In addition, the TGA mass loss at pH 2 was 3.85%, which was higher than in the previous samples. These results show the great stability of the N-A-S-H gel in the FA sample against acid attack, which remained after leaching at pH 2.

Finally, the DTG curves for the FCC mortars can be seen in Fig. 5**e**. this sample's behavior against acid attack was similar to FA, and a peak was observed at 150 °C. It was attributed to the presence of N-A-S-H at pH 7 and 4. However for the pH 2 test, (the most drastic condition), the N-A-S-H gel had completely decomposed, which is in accordance with ANC behavior.

To conclude, at pH 7 and 4 we can affirm for all the tested mortars that the first DTG peak moved to values lower than 150 °C because under these acid conditions, hydration products partially disintegrated and silica/alumina gels with significant water content were produced. Water molecules were weakly bound to the amorphous SiO_2/Al_2O_3 structure, which caused their evaporation at a lower heating temperature. Except for FA, the DTG curves for the attacked samples at pH 2 reflected that the main hydration products had almost completely decomposed.

3.3. Studies into mass loss versus consumed acid at pH 2

Mass loss and consumed acid were monitored for 120 h for each monolithic mortar specimen (40×40×10 mm^3 in size). pH was left constant at 2 by adding 1 M HNO_3 solution from the dosimeter. At the predetermined times, sheets were removed from solution and weighed. An added volume of acid was recorded *versus* the reaction time.

As in the previous ANC studies, fit equations were obtained for mass (as %) *versus* time (as h), and for the HNO_3 added volume (as mL) *versus* time (as h). The equation that was best fitted to describe the behavior of mortars is as follows:

$$y = a + bx^c$$

where y is mass (%) or the HNO_3 added volume (mL) and x is the test time (h).

Table 4 shows the experimental final values of mass (%), the HNO_3 added volume (mL), and the parameters corresponding to these fitted curves. The shape of these curves appears in Fig. 6 and Fig. 7.

The greatest mass loss and the largest HNO_3 added volume corresponded to the OPC system (2.54% and 42.95 mL, respectively), with the lowest values for FA (0.91% mass loss and 17.10 mL of added acid) when the test ended. GGBS behaved similarly to OPC, but consumed a slightly smaller HNO_3 volume (34.29 mL) and its mass loss was slightly less (2.10%). The mass loss for VCAS and FCC was 1.5% and 1.4%, respectively, and the HNO_3 added volumes were 19.82 mL and 24.45 mL, respectively.

When looking at the results obtained in this study, a certain correlation between the calcium content of the binder and acid attack resistance apparently appeared, except for FCC. This could be because the formed N-A-S-H gel (FCC cannot form C-A-S-H, because this precursor does not contain calcium) was unstable against highly acidic media. FA also forms N-A-S-H gel, but the presence of a certain amount of calcium or iron possibly favors the chemical stabilization of gel [24].

3.4. Optical microscopy studies

Fig. 8 shows the photographs obtained by optical microscopy of the surface and of cross-section of the tested mortars (after 120 h of acid attack at pH 2). The newly obtained cross-sections were sprayed with

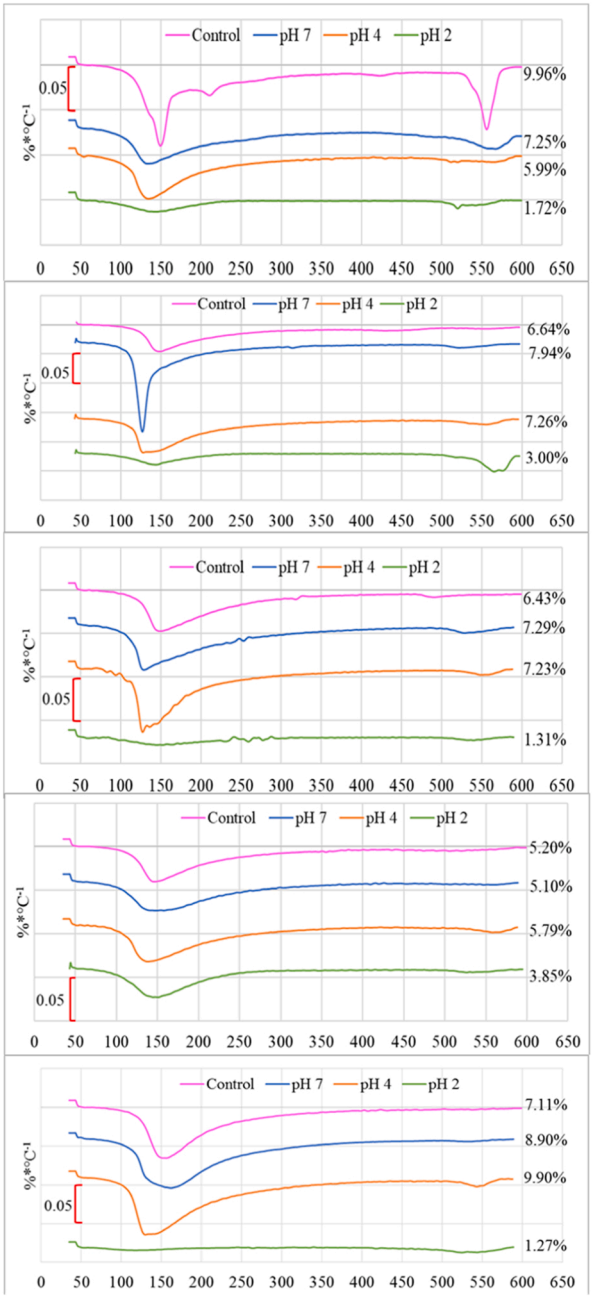

Fig. 5. DTG curves for the unattacked and attacked mortars: a) OPC; b) GGBS; c) VCAS; d) FA; e) FCC.

Table 4
Experimental results of mass (%) and the HNO3 added volume and parameters of the fitting equations *versus* time (R2 is the determination coefficient).

Material	Mass (%)	HNO_3 volume (mL)	a	b	c	R^2
OPC	97.46	–	100.33	-0.327	0.453	0.9935
	–	42.95	0	4.972	0.4504	0.9985
GGBS	97.90	–	0	100.028	-0.0045	1.00
	–	34.29	0	5.633	0.377	0.9917
VCAS	98.50	–	100.45	-0.593	0.249	0.9819
	–	19.82	0	3.400	0.368	0.9979
FA	99.09	–	100.07	-0.056	0.598	0.9007
	–	17.10	0	4.229	0.292	0.9746
FCC	98.60	–	0	100.40	-0.0038	0.9915
	–	24.45	-19.57	21.976	0.154	0.9925

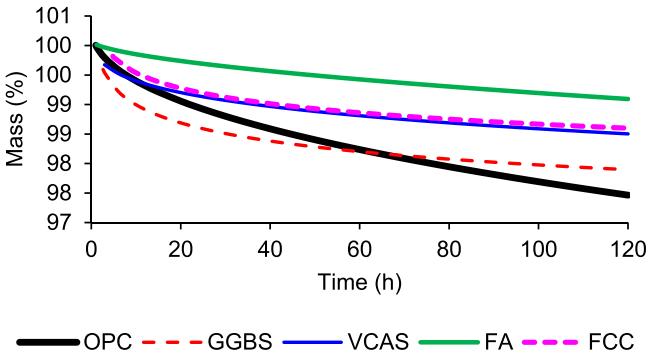

Fig. 6. Fitting curves of mass *versus* time for the mortars immersed in HNO_3 solution at a constant pH of 2.

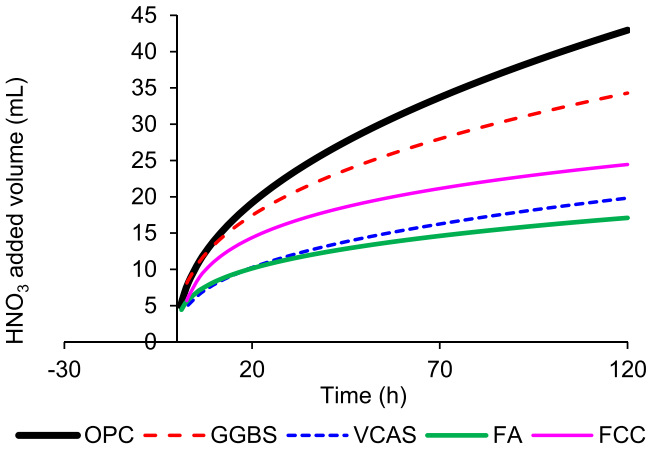

Fig. 7. Fitting curves of the HNO_3 added volume *versus* time for the mortars immersed in HNO_3 solution at a constant pH of 2.

phenolphthalein solution to visualize the degree of acid attack penetration.

The surface of the OPC specimen (Fig. 8a) showed areas attacked by the acid (light brown due to iron oxide precipitation) corresponding to the binder. Loss of paste was observed and the aggregate crumbled when handled. On the cross-section of this mortar, the attack front was less than 1 mm, which left the inside of the sample intact.

The surface of the GGBS sample (Fig. 8b) displayed some micro-cracks due to paste degradation, but its texture was more compact than that of the OPC mortar and it was not light brown (due to its low iron content). On the cross-section, there was no significant acid attack front.

The VCAS sample did not display any acid attack front on its cross-section (Fig. 8c), but the external face had a well-defined network of cracks of varying dimensions, some of which were 0.5 mm long. Most of the cementing phase remained among sand particles.

The FA surface (Fig. 8d) showed a network of longer cracks than those observed for the VCAS mortar (even 1 mm), but were much thinner and looked quite compact. Internally, there was no appreciable attack to exposure at pH 2. No significant loss of cementing phase was observed, which agrees with the results of the ANC values and the mass loss analysis.

Finally, the appearance of the attacked surface in the FCC sample (Fig. 8e) was similar to VCAS, but with fewer cracks that were longer (1 mm long). In this case, the acidic medium caused paste to shrink, which was when cracks formed. For this sample, there was no evidence for acid attack on the cross-section.

We conclude from this study that acid did not penetrate too much (except for OPC) into cementitious matrices, probably due to the short test time and the presence of the siliceous aggregate that did not allow

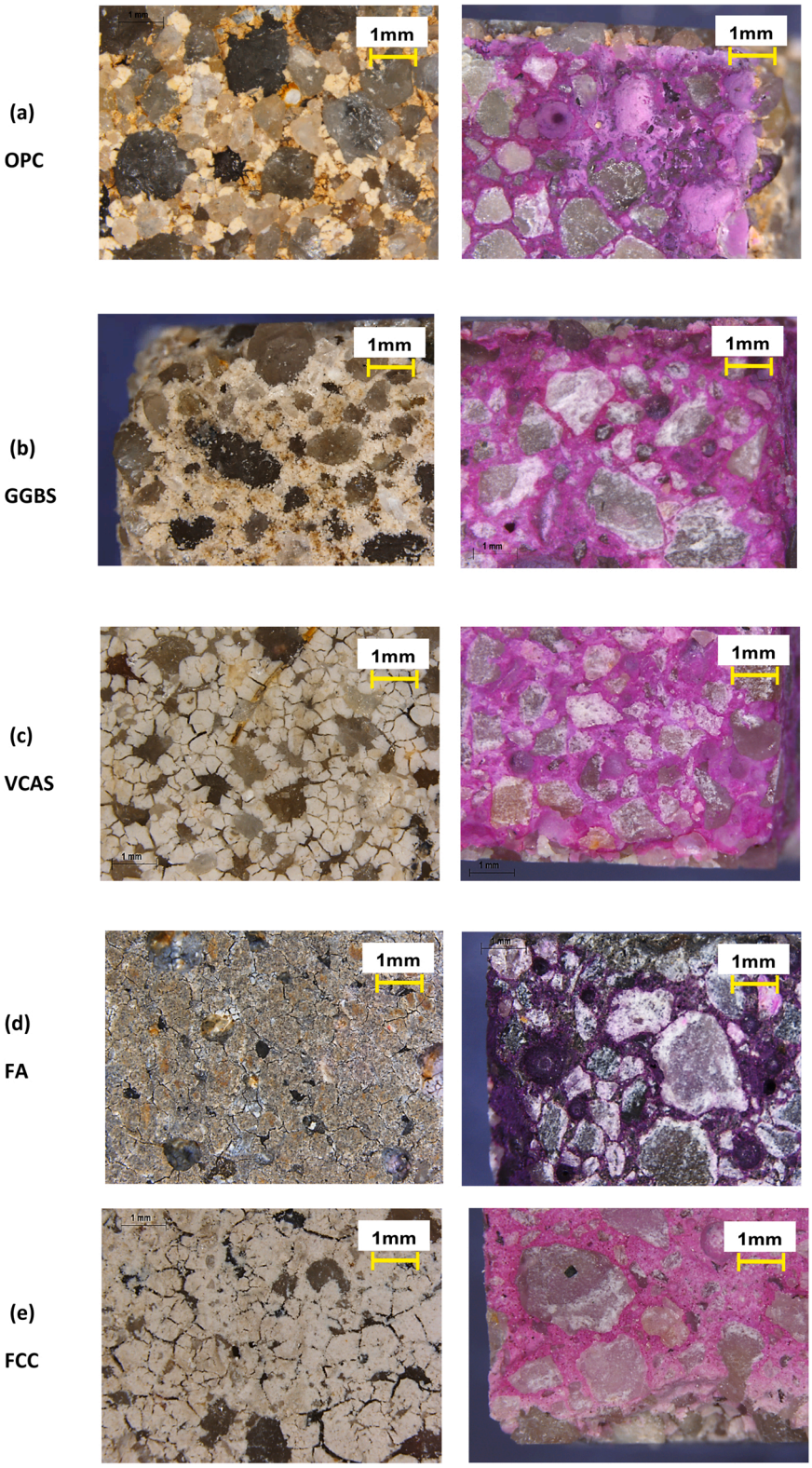

Fig. 8. Photographs taken by optical microscopy of (a) OPC, (b) GGBS, (c) VCAS, (d) FA and (e) FCC from the surface (left column) and a cross-section (right column) of the monolithic specimens attacked by HNO_3 at pH 2 for 120 h.

aggregate corrosion to considerably progress.

3.5. FESEM studies

This study was conducted only on the attacked OPC and FCC samples. The elementary mappings (oxygen was omitted for the calculated percentages. Only Ca, Si, Al and Na were considered) on the polished mortar cross-sections of these samples are shown in Fig. 9 and Fig. 10.

The OPC profile showed (Fig. 9) aggregate particles (sand) and the Si

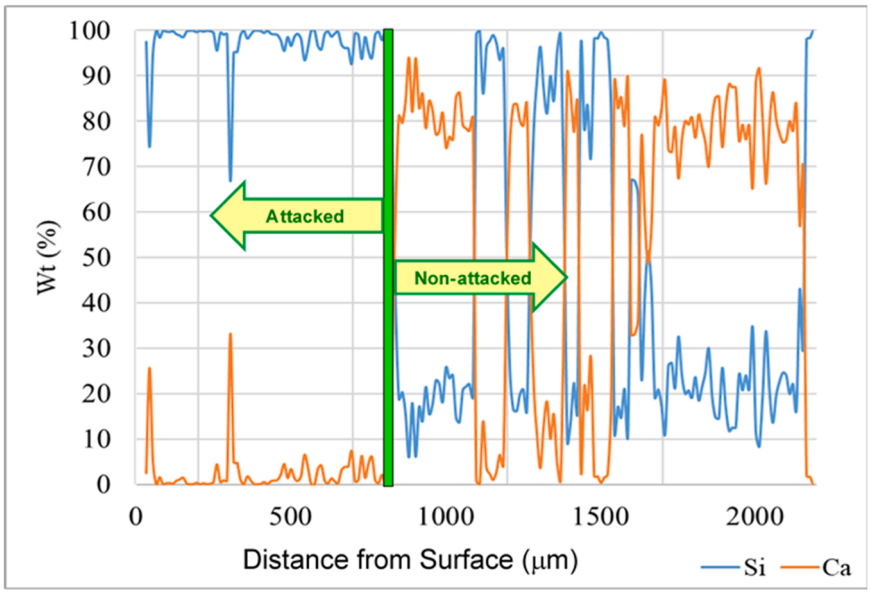

Fig. 9. Chemical elements profile (only Ca and Si) for the OPC mortar (monolithic mortar specimen attacked by HNO_3 at pH 2 for 120 h).

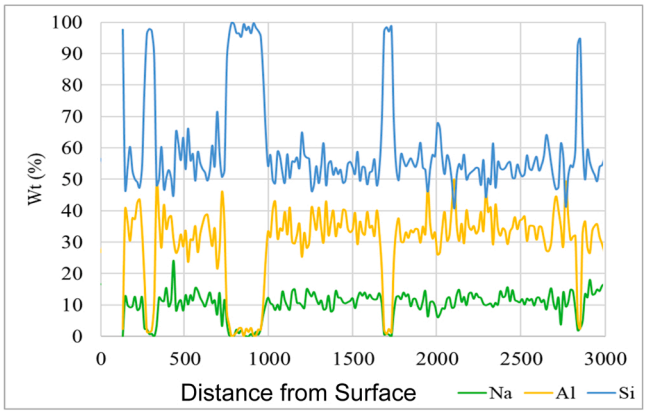

Fig. 10. Chemical elements profile (only Na, Al and Si) for the FCC mortar (monolithic mortar specimen attacked by HNO_3 at pH 2 for 120 h).

percentage was maximum, while the Ca percentage range was 60–90% and the Si range was 10–40% when there was paste. These values demonstrated the presence of the C-S-H gel. Attack slightly progressed minor, c.a. 900 μm (the zone in Fig. 9 where Ca came close to 0%, and the main element was Si from the aggregate or silica gel formed by C-S-H decomposition *via* Ca leaching). Within 1000–1500 μm range from the surface, at some points Si was 100% due to the presence of quartz particles.

Al, Si and Na can be seen on the FCC profile (Fig. 10),. This means that the N-A-S-H gel was present in the paste surrounding the aggregate particles, while lack of Al and Na and the maximum Si percentages imply the presence of aggregates. Along the analyzed profile, the positive values for the three chemical elements appear together, which suggests that the N-A-S-H gel was not attacked by acid, and Na was not leached from the gel. De-alumination and dealkalination processes did not take place under these conditions, unlike what Wang et al. [25] reported under stronger conditions for N-A-S-H.

3.6. Mass loss studies for the mortars immersed in nitric acid (initial concentration of 1 M)

In this study, the remaining mass behavior of the mortar specimens exposed to a very aggressive environment was analyzed. The cubic specimens were immersed in 1 M HNO_3 solution (initial theoretical pH of 0). The mass variation of specimens and the pH of solution were recorded over time. Six samples were tested per mortar type, which gave the corresponding average values of the remaining mass (as a %) and pH. As in previous studies, a fit equation for mass (in %) *versus* time (days) was obtained. The equation that best fitted to describe the behavior of mortars is as follows:

$$y = a\ln x + b$$

where y is mass (in %) and x is the test time (days). Table 5 shows the final experimental values of the remaining mass (%) and the parameters corresponding to these fitted curves.

Table 5
Experimental results of the remaining mass of the cubic specimens (%) and parameters of fitting equations *versus* time (R2 is the determination coefficient).

Material	Remaining mass at the end the test (%)	a	b	R^2
OPC	90.6	-1.924	96.082	0.9989
GGBS	93.3	-0.922	95.656	0.9939
VCAS	89.3	-1.325	94.531	0.9883
FA	96.2	-0.747	99.362	0.9887
FCC	61.6	-3.497	72.785	0.9582

Fig. 11 depicts the corresponding curves for the mass variations *versus* time for the tested mortars. Fig. 12 shows the variation in pH of solution *versus* time.

As seen in **Fig.- 11**, the mortar that underwent the most mass loss was FCC: 25% of its mass ws lost during the first 24 h of testing, which was a much higher percentage than those corresponding to the other mortars. This matches previous results, which found that when the pH of the medium dropped, FCC displayed worse behavior. This indicates that its hydration products lost stability as the acidic conditions of the medium increased. The mortar with the least mass loss was FA, with only 3.8% at the end of the test.

Fig. 12 shows the variation in pH *versus* the test time of the analyzed materials. It was noteworthy that OPC obtained the highest final pH value (2.77), but was not the sample with the greatest mass loss.What this, evidences is that the Ca^{+2}/OH^- ions were transferred from the matrix to the acid medium by neutralizing it. The mass loss in OPC did not further advance because the neutralization of the medium prevented

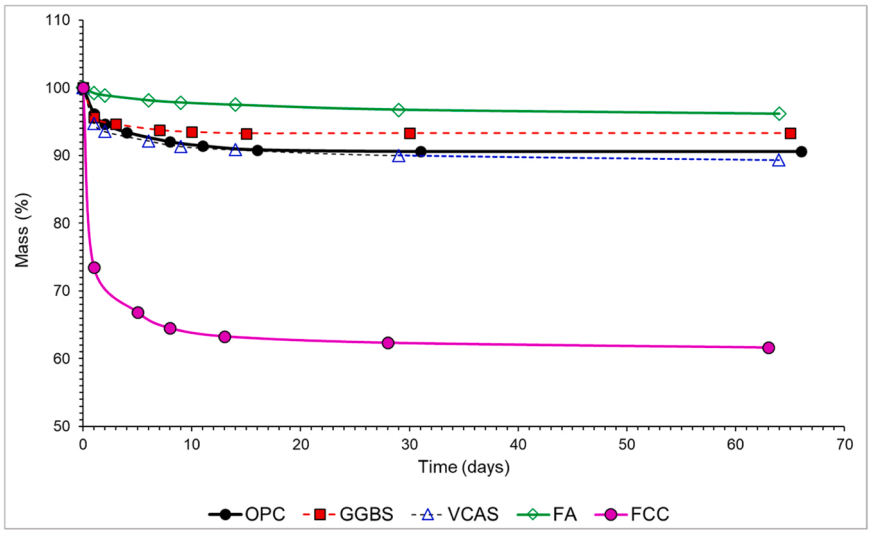

Fig. 11. Fitting curves of the remaining mass *versus* time for the cubic specimens.

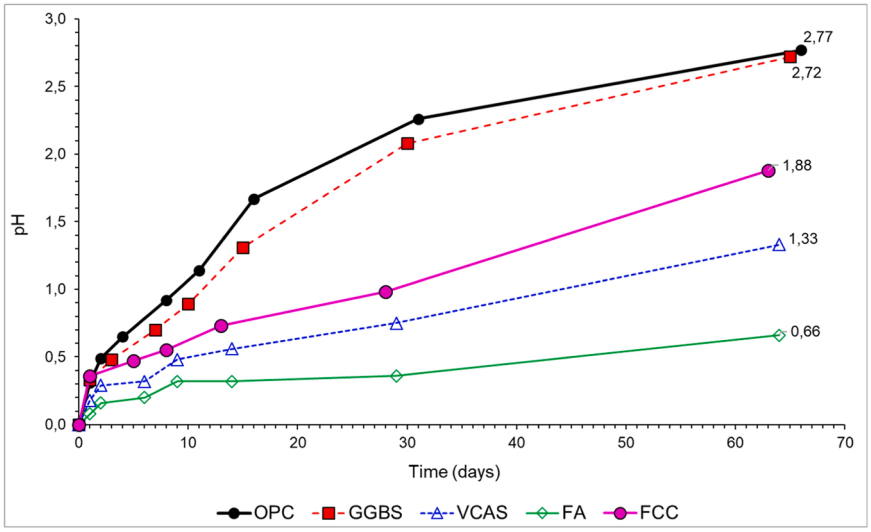

Fig. 12. Values of pH variation *versus* time for the solution in which the cubic specimens were immersed.

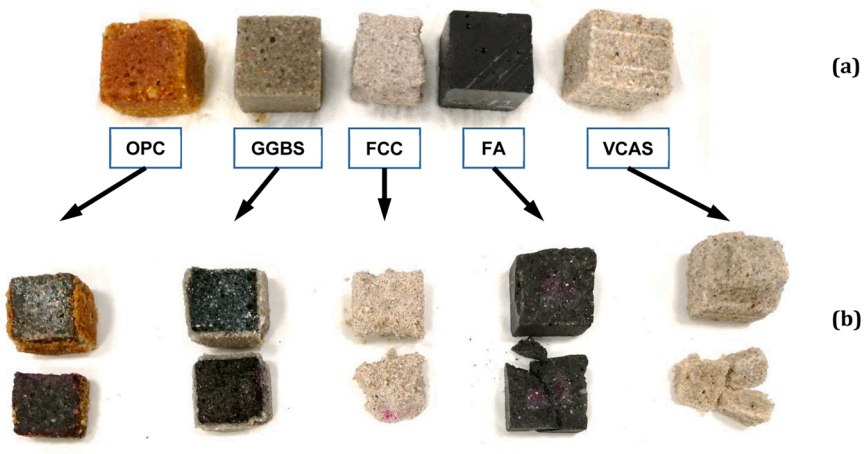

Fig.- 13. Mortar samples after being immersed in nitric acid solution for 60 days (initial pH 0); (b) cross-sections of the specimens revealed with phenolphthalein.

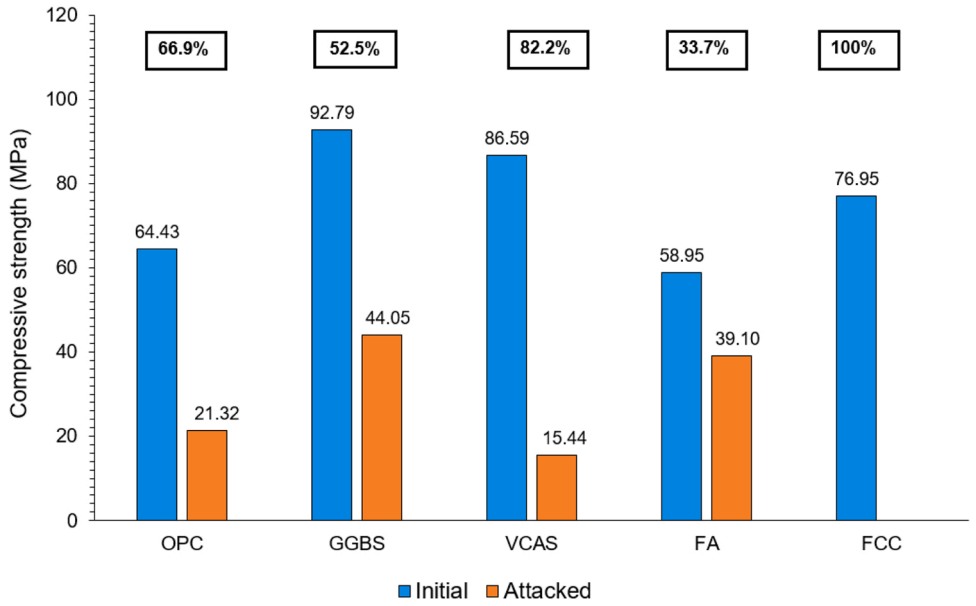

Fig. 14. Compressive strength of the pristine and attacked mortars. The values at the top correspond to the percentage of mechanical strength loss (the attacked FCC mortar was not measured because of the high mass loss that occurred).

the reaction from progressing. This agrees with its high ANC, which was measured in the first section of this research. The samples with GGBS and VCAS also were well able to neutralize the acidity of the medium with good chemical stability for the cementing gels. The FA sample displayed the greatest stability against the high acidity of the tested medium, which corroborates the strong chemical stability of the N-A-S-H gel present in this geopolymer type. Conversely, FCC showed more acid consumption during the neutralization process, and its mass loss was marked when the nature of the cementing gel of the N-A-S-H type was not taken into account Probably, with this very acidic medium, de-alumination progressed [25] and the gel became unstable.

The greatest mass loss and change in the aspect of mortars occurred on the first 7 days of immersion in acid solution, but then they hardly changed until the end of the experiment at 60 days. The aspect of specimens after the test ended appears in Fig. 13a. The reddish color of the OPC sample was due to the presence of Fe^{+3} compounds. The OPC and GGBS samples displayed intense surface deterioration due to their higher Ca content. The FCC sample underwent the most deterioration and the greatest mass loss. The FA sample had the best visual appearance, which is consistent with its least mass loss. For each tested mortar, a cubic specimen was selected, cut in half and revealed with phenolphthalein to observe the acid attack front (Fig. 13b). The results were as follows: OPC 4.5 mm, GGBS 3.25 mm and FA 9.8 mm, measured from the specimen surface. The FCC and VCAS samples showed no pink color when revealed with the indicator, probably because the initial pH (before acid attack) was below 10.

Finally, the compressive strength of the attacked mortars was measured and compared to the compressive strength of the unattacked mortars. Fig. 14 shows the results of these measurements (average of three samples) and indicates the percentage of loss of strength between the pristine mortars and those attacked. It was verified that lower mechanical strength loss corresponded to the FA mortar (33.68%), which is indicative of the good stability of the N-A-S-H gel against acid attack.

4. Conclusions

Alkali-activated mortars (AAMs) were tested for acid attack by nitric acid solutions. The following conclusions are drawn:

a) The ANC values are generally higher when the calcium content of the binder increases. This behavior demonstrates the greater stability of the alkali-activated system compared to the OPC mortar. Only the FCC mortar behaves worse at pH 2 because the reaction products could contain some reactive phases at such a low pH.
b) A mathematical model is proposed to fit acid consumption (mmol H^+/g of mortar) *versus* the testing time.
c) The stability of the alkali-activated system is corroborated by a TGA of the samples at the end of the ANC test. The N-A-S-H gel is present in many cases after acid attack, whereas the C-S-H and C-A-S-H gels are decomposed.
d) Mortar sheets show less mass loss upon an acid attack at pH 2 for the alkali-activated systems, especially for those with low calcium content in the precursor. This behavior agrees with ANC trends.
e) A strong acid attack by immersion in 1 M nitric acid solution is very aggressive for all the tested samples: a marked drop in mortar compressive strength is recorded. However, the FA system shows the best behavior because of high N-A-S-H gel stability.

The proposed test, based on three complementary experiments (acid neutralization capacity, mass loss in mortars subjected to constant a pH of 2 and mass loss of the mortar cubes immersed in 1 M nitric acid) allows the analysis of AAMs´ stability and the identification more resistant systems to acid attack.

Declaration of Competing Interest

The authors declare the following financial interests/personal relationships which may be considered as potential competing interests. Jordi Paya reports financial support was provided by Universitat Politècnica de València.

Data Availability

Data will be made available on request.

References

[1] I. García-Lodeiro, A. Fernández-Jiménez, A. Palomo, Variation in hybrid cements over time. Alkaline activation of fly ash–portland cement blends, Cem. Concr. Res. 52 (2013) 112–122, https://doi.org/10.1016/j.cemconres.2013.03.022.

[2] Y.H. Mugahed Amran, R. Alyousef, H. Alabduljabbar, M. El-Zeadani, Clean production and properties of geopolymer concrete: a review, J. Clean. Prod. 251 (2020), 119679, https://doi.org/10.1016/j.jclepro.2019.119679.
[3] N.B. Singh, B. Middendorf, Geopolymers as an alternative to Portland cement: an overview, Constr. Build. Mater. 237 (2020), 117455, https://doi.org/10.1016/j.conbuildmat.2019.117455.
[4] P.V. Krivenko, V.G. Bashtovoi, Geopolymer materials based on power station fly ash, J. Build. Mater. Struct. 2 (2016) 50–55.
[5] Z. Zhang, X. Yao, X. Qiu, C. Wu, S. Wu, Z. Zhang, The effect of curing temperature on the mechanical properties of fly ash-based geopolymer, Adv. Mater. Sci. Eng. (2018) 1–10.
[6] M. Criado, A. Palomo, A. Fernández-Jiménez, Alkali-activated fly ashes: a cement for the future, Cem. Concr. Res. 38 (2008) 864–876, https://doi.org/10.1016/S0008-8846(98)00243-9.
[7] A. Singhal, S. Gupta, Fly ash-based geopolymer: a review, J. Build. Eng. 19 (2018) 412–419.
[8] C. Shi, P.V. Krivenko, Alkali-activated slag and slag blends: a review, Materials 9 (2016) 951.
[9] N.T. Sithole, T. Mashifana, Geosynthesis of building and construction materials through alkaline activation of granulated blast furnace slag, Constr. Build. Mater. 264 (2020), 120712, https://doi.org/10.1016/j.conbuildmat.2020.120712.
[10] M.M. Tashima, J.L. Akasaki, V.N. Castaldelli, L. Soriano, J. Monzó, J. Payá, M. V. Borrachero, New geopolymeric binder based on fluid catalytic cracking catalyst residue (FCC), Mater. Lett. 80 (2012) 50–52, https://doi.org/10.1016/j.matlet.2012.04.051.
[11] M.M. Tashima, L. Soriano Martinez, J.M. Monzó Balbuena, M.V. Borrachero Rosado, J.J. Paya Bernabeu, Novel geopolymeric material cured at room temperature, Adv. Appl. Ceram. 112 (2013) 179–183, https://doi.org/10.1179/1743676112Y.0000000056.
[12] V. Živica, A. Bajza, Acidic Attack of Cement Based Materials—A Review. Part 1. Principle of Acidic Attack, Constr. Build. Mater. 15 (2001) 331–340, https://doi.org/10.1016/S0950-0618(01)00012-5.
[13] V. Živica, A. Bajza, Acidic attack of cement based materials – a review. Part 2. Factors of rate of acidic attack and protective measures, Constr. Build. Mater. 16 (2002) 215–222, https://doi.org/10.1016/S0950-0618(02)00011-9.
[14] Q. Chen, L. Zhang, Y. Ke, C. Hills, Y. Kang, Influence of carbonation on the acid neutralization capacity of cements and cement-solidified/stabilized electroplating sludge, Chemosphere 74 (2009) 758–764, https://doi.org/10.1016/j.chemosphere.2008.10.044.
[15] T. Damion, P. Chaunsali, Evaluating acid resistance of Portland cement, calcium aluminate cement, and calcium sulfoaluminate based cement using acid neutralization, Cem. Concr. Res. 162 (2022), 107000, https://doi.org/10.1016/j.cemconres.2022.107000.
[16] S. Prashanth, B. Vijayalaxmi Kedilaya, Can geopolymer concrete replace the conventional concrete? State of the Art. Sustain. Constr. Build Mater. Lecture Notes in Civil Engineering 25, Springer,, 2019, https://doi.org/10.1007/978-981-13-3317-0_72.
[17] K. Arbi, M. Nedeljkovic, Y. Zuo, G. Ye, A review on the durability of alkali-activated fly-ash/slag systems: advances, issues and perspectives, Eng. Chem. Res. 55 (2016) 5439–5453, https://doi.org/10.1021/acs.iecr.6b00559.
[18] G. Mallikarjuna Rao, C.H. Kireety, Durability Studies on Alkali Activated Fly Ash and GGBS-Based Geopolymer Mortars, Sustain. Constr. Build. Mater. Lecture Notes in Civil Engineering 25 (2019) Springer. https://doi.org/10.1007/978-981-13-3317-0_8.
[19] A. Mellado, M.I. Pérez-Ramos, J. Monzó, M.V. Borrachero, J. Payá, Resistance to acid attack of alkali-activated binders: Simple new techniques to measure susceptibility, Constr. Build. Mater. 150 (2017) 355–366, https://doi.org/10.1016/j.conbuildmat.2017.05.224.
[20] M.M. Hossain, M.R. Karim, M.K. Hossain, M.N. Islam, M.F.M. Zain, Durability of mortar and concrete containing alkali-activated binder with pozzolans: a review, Constr. Build. Mater. 93 (2015) 95–109, https://doi.org/10.1016/j.conbuildmat.2015.05.094.
[21] R.R. Lloyd, J.L. Provis, J.S.J. van Deventer, Acid resistance of inorganic polymer binders. 1. Corrosion rate, Mater. Struct. 45 (2012) 1–14, https://doi.org/10.1617/s11527-011-9744-7.
[22] EA NEN 7371:2004, Leaching characteristics of granular building and waste materials. The determination of the availability of inorganic components for leaching. The maximum availability leaching test, Environment Agency, Version 1.0, April 2005.
[23] Y. Yamazaki, J. Kim, K. Kadoya, Y. Hama, Physical and chemical relationships in accelerated carbonation conditions of alkali-activated cement based on type of binder and alkali activator, Polymers 13 (2021) 671, https://doi.org/10.3390/polym13040671.
[24] M. Kaya, F. Koksal, O. Gencel, M.J. Munir, S.M.S. Kazmi, Influence of micro Fe_2O_3 and MgO on the physical and mechanical properties of the zeolite and kaolin based geopolymer mortar, J. Build. Eng. 52 (2022), 104443, https://doi.org/10.1016/j.jobe.2022.104443.
[25] Y. Wang, Y. Cao, Z. Zhang, J. Huang, P. Zhang, Y. Ma, H. Wang, Study of acidic degradation of alkali-activated materials using synthetic C-(N)-A-S-H and N-A-S-H gels, Compos. Part B: Eng. 230 (2022), 109510, https://doi.org/10.1016/j.compositesb.2021.109510.